Angiotensin II (AT1) Receptors and NADPH Oxidase Regulate Cl⁻ Current Elicited by β1 Integrin Stretch in Rabbit Ventricular Myocytes

DAVID M. BROWE[1] AND CLIVE M. BAUMGARTEN[1,2]

[1]Department of Physiology and [2]Department of Internal Medicine (Cardiology), Medical College of Virginia, Virginia Commonwealth University, Richmond, VA 23298

ABSTRACT Direct stretch of β1 integrin activates an outwardly rectifying, tamoxifen-sensitive Cl⁻ current (Cl⁻ SAC) via focal adhesion kinase (FAK) and/or Src. The characteristics of Cl⁻ SAC resemble those of the volume-sensitive Cl⁻ current, $I_{Cl,swell}$. Because myocyte stretch releases angiotensin II (AngII), which binds AT1 receptors (AT1R) and stimulates FAK and Src in an autocrine-paracrine loop, we tested whether AT1R and their downstream signaling cascade participate in mechanotransduction. Paramagnetic beads coated with mAb for β1-integrin were applied to myocytes and pulled upward with an electromagnet while recording whole-cell anion current. Losartan (5 μM), an AT1R competitive antagonist, blocked Cl⁻ SAC but did not significantly alter the background Cl⁻ current in the absence of integrin stretch. AT1R signaling is mediated largely by H_2O_2 produced from superoxide generated by sarcolemmal NADPH oxidase. Diphenyleneiodonium (DPI, 60 μM), a potent NADPH oxidase inhibitor, rapidly and completely blocked both Cl⁻ SAC elicited by stretch and the background Cl⁻ current. A structurally unrelated NADPH oxidase inhibitor, 4-(2-aminoethyl) benzenesulfonyl fluoride (AEBSF, 0.5 and 2 mM), also rapidly and completely blocked Cl⁻ SAC as well as a large fraction of the background Cl⁻ current. With continuing integrin stretch, Cl⁻ SAC recovered upon washout of AEBSF (2 mM). In the absence of stretch, exogenous AngII (5 nM) activated an outwardly rectifying Cl⁻ current that was rapidly and completely blocked by DPI (60 μM). Moreover, exogenous H_2O_2 (10, 100, and 500 μM), the eventual product of NADPH oxidase activity, also activated Cl⁻ SAC in the absence of stretch, whereas catalase (1,000 U/ml), an H_2O_2 scavenger, attenuated the response to stretch. Application of H_2O_2 during NADPH oxidase inhibition by either DPI (60 μM) or AEBSF (0.5 mM) did not fully reactivate Cl⁻ SAC, however. These results suggest that stretch of β1-integrin in cardiac myocytes elicits Cl⁻ SAC by activating AT1R and NADPH oxidase and, thereby, producing reactive oxygen species. In addition, NADPH oxidase may be intimately coupled to the channel responsible for Cl⁻ SAC, providing a second regulatory pathway.

KEY WORDS: stretch-activated channels • swelling-activated channels • arrhythmia • preconditioning • heart failure

INTRODUCTION

Integrins are heterodimeric receptors for the extracellular matrix that physiologically transmit forces from the extracellular matrix to the cytoskeleton and participate in signaling (Wang et al., 1993; Ross and Borg, 2001). We recently showed that direct stretch of β1-integrin using mAb-coated paramagnetic beads evokes an outwardly rectifying Cl⁻ current (Cl⁻ SAC) in rabbit ventricular myocytes (Browe and Baumgarten, 2003b), whereas several other forms of stretch do not stimulate Cl⁻ currents (Baumgarten and Clemo, 2003; Browe and Baumgarten, 2003b). Mechanotransduction involves protein tyrosine kinases (PTKs), specifically focal adhesion kinase (FAK) and/or Src, the principal upstream PTKs stimulated by both mechanical stretch (Sadoshima and Izumo, 1997) and integrin clustering (Parsons, 2003). Cl⁻ SAC resembles $I_{Cl,swell}$, the volume-sensitive

Cl⁻ current elicited in cardiac myocytes by osmotic swelling (Tseng, 1992; Sorota, 1992) or hydrostatic pressure-induced cell inflation (Hagiwara et al., 1992). Like $I_{Cl,swell}$, Cl⁻ SAC activates slowly over several minutes, exhibits outward rectification, partially inactivates at positive potentials, and is blocked by tamoxifen (Browe and Baumgarten, 2003b). Furthermore, $I_{Cl,swell}$ is regulated by PTKs (Sorota, 1995), including Src (Lepple-Wienhues et al., 2000), and other signaling molecules activated by stretch or integrin clustering, such as PKC (Duan et al., 1995), protein phosphatases (Duan et al., 1999), phosphatidylinositol-3-kinase (PI-3K) (Shi et al., 2002), and small GTP-binding proteins (Tilly et al., 1996; Nilius et al., 1999).

Stretch of cardiac myocytes causes the rapid release of angiotensin II (AngII), which stimulates the G pro-

---

Address correspondence to Clive M. Baumgarten, Department of Physiology, Medical College of Virginia, Box 980551, Richmond, VA 23298-0551. Fax: (804) 828-7382; email: clive.baumgarten@vcu.edu

---

Abbreviations used in this paper: AEBSF, 4-(2-aminoethyl) benzenesulfonyl fluoride; AngII, angiotensin II; DPI, diphenyleneiodonium; cSOD, extracellular-facing SOD; FAK, focal adhesion kinase; PI-3K, phosphatidylinositol-3-kinase; PTK, protein tyrosine kinase; ROS, reactive oxygen species; SOD, superoxide dismutase.

tein–coupled AT1 receptor in an autocrine–paracrine loop (Sadoshima et al., 1993). Subsequently, AT1 receptors initiate the activation of FAK, Src, PKC, protein phosphatases, PI-3K, and small GTP-binding proteins (Seshiah et al., 2002; Touyz, 2002). These are the same signaling molecules that are activated by integrin clustering, and in turn, regulate Cl^- SAC and/or $I_{Cl,swell}$. Furthermore, AngII elicits an outwardly rectifying Cl^- current in rabbit ventricular (Morita et al., 1995) and sino-atrial node (Bescond et al., 1994) myocytes. The AngII-stimulated Cl^- current in sino-atrial node is regulated by PKC and blocked by losartan, a nonpeptide specific AT1 receptor antagonist (Bescond et al., 1994). Taken together, these data raise the possibility that AT1 receptors are involved in the activation of Cl^- SAC by β1-integrin stretch.

AngII-induced signaling is mediated largely by reactive oxygen species (ROS) generated by sarcolemmal NADPH oxidase, a heteromeric enzyme complex broadly distributed throughout cardiovascular and other tissues (Griendling et al., 2000; Vignais, 2002). Cardiac myocytes express all of the components of a phagocyte-like NADPH oxidase: a transmembrane flavocytochrome b_{558} complex consisting of a large gp91^{phox} (Nox2) and a smaller p22^{phox} subunit, cytosolic p47^{phox} and p67^{phox} subunits, and the small GTP-binding protein Rac (Li et al., 2002; Xiao et al., 2002; Heymes et al., 2003). Nox4, a gp91^{phox} homologue, recently was found to be expressed as well (Byrne et al., 2003). Translocation of the cytosolic subunits and Rac to the membrane and their assembly with gp91^{phox} and p22^{phox} involves PKC, Src and other PTKs, and PI-3K (Yamaguchi et al., 1996; Bokoch and Diebold, 2002; Seshiah et al., 2002; Vignais, 2002). Once activated, the phagocyte-type NADPH oxidase uses intracellular NADPH and NADH as electron donors to catalyze the single electron reduction of extracellular molecular oxygen to superoxide anion ($O_2^-\cdot$) (Griendling et al., 2000; Vignais, 2002). $O_2^-\cdot$ is unstable and is rapidly converted by superoxide dismutase (SOD) to H_2O_2, a more stable, membrane-permeant ROS that widely participates in signaling (Griendling and Ushio-Fukai, 2000) and directly activates NADPH oxidase (Grandvaux et al., 2001; Li et al., 2001). In ventricular myocytes, dismutation is performed by membrane-bound extracellular-facing SOD (ecSOD), as well as cytoplasmic CuZn and mitochondrial Mn isoforms of SOD (Brahmajothi and Campbell, 1999).

The aim of the present study was to test the hypothesis that the AT1 receptor-NADPH oxidase-H_2O_2 signaling pathway participates in the activation of Cl^- SAC by stretch of β1-integrin in ventricular myocytes. Paramagnetic beads coated with anti-β1-integrin mAb were employed to specifically stretch integrins. Block of either the AT1 receptor or NADPH oxidase and also enzy-

matic scavenging of H_2O_2 during stretch inhibit Cl^- SAC. Furthermore, either AngII or H_2O_2 applied in the absence of stretch activate Cl^- SAC. Preliminary reports appeared previously (Browe and Baumgarten, 2003a, 2004).

MATERIALS AND METHODS

Ventricular Myocyte Isolation

Left ventricular myocytes were freshly isolated from adult New Zealand white rabbits (∼3 kg) by a pronase-collagenase II enzymatic dissociation procedure as described previously (Browe and Baumgarten, 2003b) and stored in a modified KB medium. All membrane current recordings were made within 10 h after myocyte isolation. Single myocytes chosen for study were rod-shaped, quiescent, displayed clear striations, and were free of membrane blebs or other morphological irregularities.

Tyrode solution for cell isolation contained (in mM) 130 NaCl, 5 KCl, 1.8 CaCl$_2$, 0.4 KH$_2$PO$_4$, 3 MgCl$_2$, 5 HEPES, 15 taurine, 5 creatine, 10 glucose, pH 7.25. For Ca-free Tyrode solution, CaCl$_2$ was replaced with 0.1 mM Na$_2$EGTA. For enzyme solution, 1.5–1.75 mg/ml BSA (Sigma-Aldrich), 0.5 mg/ml collagenase (type II; Worthington), and 0.05 mg/ml pronase (type XIV; Sigma-Aldrich) were added to Ca- and EGTA-free Tyrode. KB solution contained (in mM) 120 K-glutamate, 10 KCl, 10 KH$_2$PO$_4$, 0.5 K$_2$EGTA, 10 taurine, 1.8 MgSO$_4$, 10 HEPES, 20 glucose, 10 mannitol, pH 7.2.

Experimental Solutions and Drugs

Single ventricular myocytes were scattered on a poly-L-lysine–coated, glass-bottomed chamber and placed on the stage of an inverted microscope (Diaphot; Nikon). Hoffman modulation optics (×40; NA = 0.55) and a high resolution TV camera (CCD72; Dage-MTI) were used to visualize myocytes. Bath solution designed to isolate anion currents was suprafused at 2–3 ml/min and contained (in mM) 145 N-methyl-D-glucamine (NMDG)-Cl, 4.3 MgCl$_2$, 10 HEPES, 5 glucose, pH 7.4. The pipette solution contained (in mM) 110 Cs-aspartate, 20 CsCl, 2.5 MgATP, 8 Cs$_2$EGTA, 0.1 CaCl$_2$, 10 HEPES, pH 7.1 (liquid junction potential, −13.2 mV). Pipette free-Ca^{2+} was estimated as ∼35 nM (WinMAXC ver 2.4; www.stanford.edu/~cpatton/maxc.html). All recordings were made at room temperature (22–23°C).

Tamoxifen (20 mM; Sigma-Aldrich) was prepared as a stock solution in DMSO and kept frozen (−4°C) in small aliquots until use. Diphenyleneiodonium chloride (DPI; Sigma-Aldrich) was dissolved by warming in DMSO and added to bath solution. The final concentration of DMSO was 0.1%. Losartan-K (Merck), 4-(2-aminoethyl)-benzenesulfonyl fluoride HCl (AEBSF; Sigma-Aldrich), and catalase (Sigma-Aldrich) were dissolved directly in bath solution. Human AngII (Calbiochem) was dissolved in 5% acetic acid, but its addition to bath solution did not significantly alter pH. H_2O_2-containing solutions were freshly prepared by diluting 30% (wt/wt) H_2O_2 (Fisher Scientific) to make a 10 mM stock that was added to bath solution.

Paramagnetic Bead Method

As previously described (Browe and Baumgarten, 2003b), stretch was applied directly and specifically to β1-integrins with mAb-coated paramagnetic beads and an electromagnet. IgG$_1$ mAb for the β1 subunit of integrin (MAB2250; Chemicon) was attached by an anti-pan IgG mAb to the surface of uniform 4.5 ± 0.2 μm diameter (mean ± SD) superparamagnetic beads containing iron oxides (Dynabeads M-450 Pan Mouse IgG; Dynal Biotech).

Anti-β1-integrin mAb–coated beads were added to myocytes in the experimental bath and permitted to randomly settle on myocytes from above while the flow of bath solution was turned off. After ~5 min, unbound beads were washed away by restoring bath flow. Myocytes chosen for study typically had three to five coated beads on their surface, and presumably, each bead was bound to multiple β1 integrins.

An electromagnet was placed directly on top of the experimental bath, and patch pipettes were passed through an elliptical opening at its base. Coil current was set to generate a magnetic flux density of 35 Gauss (G) and a magnetic flux density gradient of 2,400 G/m that was uniform in the x–y plane occupied by the myocytes (5080 Gauss meter; F.W. Bell). The resulting force vector imposed on each bead was directed upwards toward the coil, perpendicular to the long axis of the myocyte, and was estimated to have a magnitude of 1.2 pN/bead (Browe and Baumgarten, 2003b).

Electrophysiological Recordings

Pipettes were pulled from 7740 thin-walled borosilicate glass capillary tubing and then fire polished to give a final tip diameter of 3–4 μm and resistance in bath solution of 2–3 MΩ. Membrane currents were recorded with an EPC-7 amplifier (List-Medical) using the whole cell configuration of the patch clamp technique. A 150 mM KCl agar bridge served as the ground electrode during recordings. Seal resistances of 5–30 GΩ were typically obtained. Membrane potential was corrected for the measured liquid junction potential before forming a seal. The membrane patch was ruptured by a brief, 500-mV zapping pulse, and myocytes were dialyzed for 10 min before recordings commenced. Voltage clamp protocols and data acquisition were governed by a Digidata 1200B A/D board and pClamp 8.0 (Axon Instruments). Successive 500-ms voltage steps were taken from a holding potential of −60 mV to test potentials ranging from −100 to +40 mV in +10-mV increments. Membrane currents were low-pass filtered at 2 kHz (8-pole Bessel 902; Frequency Devices) and digitized at 10 kHz. For presentation, selected records were filtered at 50 Hz. Cl⁻ SAC exhibited strong voltage-dependent inactivation, and isochronal IV curves were plotted based on the average current recorded 20–35 ms after the onset of the voltage step.

Statistics

Data are reported as mean ± SEM; n denotes the number of cells. Mean currents are expressed as current density (pA/pF) to account for differences in myocyte surface membrane area. For multiple comparisons, a repeated measures or one-way ANOVA was performed, and the Student-Newman-Keuls or the Bonferroni t test was employed to compare groups. For comparisons of two groups, a one-tailed paired Student's t test was conducted. Statistical analyses were performed by SigmaStat 2.03 (Systat), and $P < 0.05$ was taken as significant.

R E S U L T S

AT1 Receptors Participate in the Activation of Cl⁻ SAC by β1-Integrin Stretch

Mechanical stretch of myocytes releases AngII, which binds to AT1 receptors and activates FAK and Src in an autocrine–paracrine loop (Sadoshima et al., 1993). Therefore, losartan, a selective AT1 receptor competitive antagonist (Chung and Unger, 1998), was used to test whether AT1 receptors participate in the FAK-
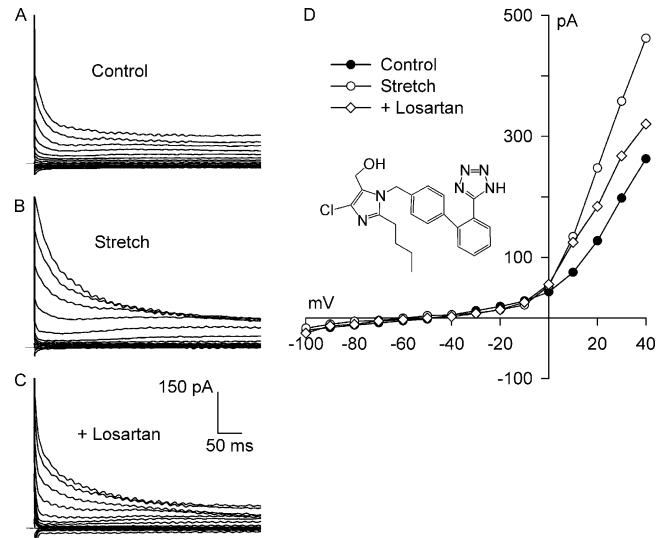

FIGURE 1. Losartan, a specific AT1 receptor competitive antagonist, inhibits Cl⁻ SAC. Membrane potential was stepped from −60 mV to test potentials between −100 and +40 mV for 500 ms in solutions designed to isolate anion currents. Membrane current families recorded before (A, Control) and after (B, Stretch) 8 min of integrin stretch, and following application of 5 μM losartan for 30 min while maintaining integrin stretch (C, +Losartan). Horizontal bar denotes 0 current. (D) I–V relationships for A–C. Each reversed near E_{Cl}. At +40 mV, the stretch-activated current was 1.15 ± 0.22 pA/pF, and losartan blocked 72 ± 3% ($n = 4$) of Cl⁻ SAC. Inset, chemical structure of losartan.

and/or Src-dependent activation of Cl⁻ SAC upon β1-integrin stretch (Browe and Baumgarten, 2003b).

Fig. 1 shows an example of families of currents obtained upon stepping voltages to between −100 and +40 mV for 500 ms, and the corresponding I–V relationships. Under control conditions in solutions designed to isolate anion currents (Fig. 1 A), a small background current that partially inactivated at potentials positive to +10 mV was present before the application of integrin stretch. The I–V relationship for the background current displayed outward-going rectification and reversed at −50 mV, near the calculated value of E_{Cl}, −52 mV (Fig. 1 D). Static stretch of the bead-attached β1-integrins for 8 min progressively increased the Cl⁻ current. The Cl⁻ current after stretch (Fig. 1 B) also partially inactivated at potentials positive to +10 mV, and its I–V relationship showed strong outward rectification and reversed at −52 mV (Fig. 1 D). The stretch-induced activation of Cl⁻ current was inhibited by selective block of AT1 receptors. Myocytes were exposed to 5 μM losartan for 30 min while maintaining stretch. After AT1 receptor blockade, the family of currents (Fig. 1 C) and the I–V relationship (Fig. 1 D) were nearly restored to their control levels.

Overall, 5 μM losartan applied for 30–32 min with continued stretch inhibited 72 ± 3% ($n = 4$; $P = 0.002$) of the Cl⁻ SAC at +40 mV. Stretch significantly
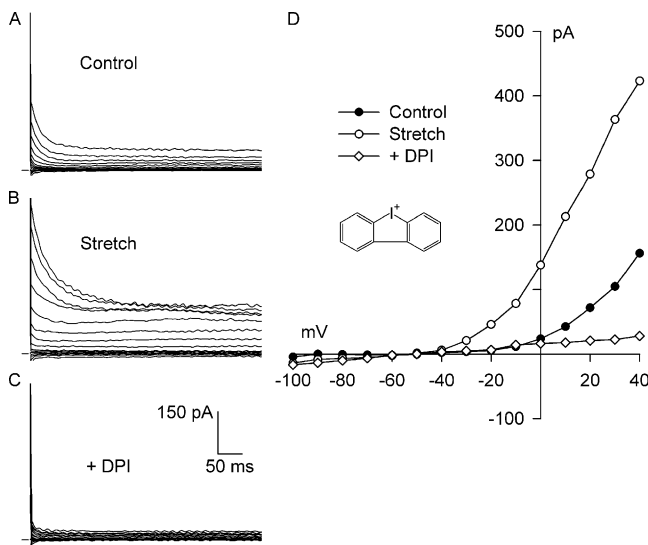
FIGURE 2. Diphenyleneiodonium (DPI), a potent inhibitor of electron transport within the NADPH oxidase complex, completely blocks both Cl⁻ SAC and background Cl⁻ current. Currents before (A, Control) and after (B, Stretch) activation of Cl⁻ SAC by 8 min of integrin stretch, and after application of 60 μM DPI for 5 min with continued stretch (C, +DPI). (D) I–V relationships for A–C, with each reversing at about −50 mV. At +40 mV, DPI blocked 156 ± 9% ($n = 6$) of the integrin stretch–induced current. The membrane current after DPI exhibited a linear I–V relationship and was significantly less than the background Cl⁻ current ($P < 0.001$ at +40 mV). Inset, chemical structure of DPI.

increased the current at +40 mV from 1.97 ± 0.15 to 3.12 ± 0.29 pA/pF, and after block of AT1 receptors, the current was reduced to 2.30 ± 0.18 pA/pF, a value not significantly different from control ($P = 0.08$, $n = 4$). At −100 mV, the stretch-induced inward currents were much smaller than the outward currents, and the control, stretch, and stretch plus losartan currents at −100 mV were not significantly different from each other ($P = 0.363$).

To verify that losartan was principally inhibiting the stretch-induced current rather than the background current, 100 μM losartan was applied for 12–15 min to unstretched myocytes that had bound anti-β1-integrin mAb-coated beads. Blockade of AT1 receptors under these conditions did not significantly alter the membrane current ($n = 4$; unpublished data).

NADPH Oxidase and H_2O_2 Participate in the Activation of Cl⁻ SAC

Activation of AT1 receptors generates ROS primarily by stimulation of the sarcolemmal NADPH oxidase (Seshiah et al., 2002). Moreover, mechanical stretch or integrin clustering can also generate ROS via activation of NADPH oxidase (Howard et al., 1997; Löfgren et al., 1999; Pimentel et al., 2001; Oeckler et al., 2003). Therefore, we tested the idea that the NADPH oxidase–

mediated generation of ROS regulates the Cl⁻ SAC elicited by integrin stretch.

Fig. 2 shows the effect of DPI, a potent inhibitor of $O_2^-\cdot$ production by NADPH oxidase that binds to the flavin and heme b redox centers of gp91^{phox} (O'Donnell et al., 1993; Doussiere et al., 1999). As before, a small, outwardly rectifying background Cl⁻ current was present before stretch (Fig. 2, A and D), and 8 min of integrin stretch greatly increased the Cl⁻ current (Fig. 2, B and D). In the continued presence of integrin stretch, exposure to 60 μM DPI for 5 min completely blocked both the Cl⁻ SAC and nearly all of the outwardly rectifying background Cl⁻ current. The current remaining after block by DPI (Fig. 2, C and D) was very small in amplitude and exhibited a linear I–V relationship.

DPI profoundly inhibited the Cl⁻ SAC as well as the background Cl⁻ current in each myocyte studied. At +40 mV, 60 μM DPI inhibited 156 ± 9% ($n = 6$, $P < 0.001$) of the Cl⁻ SAC after 5 min. In these myocytes, integrin stretch significantly increased the Cl⁻ current from 0.97 ± 0.07 to 2.04 ± 0.12 pA/pF, and DPI markedly decreased the current to 0.44 ± 0.08 pA/pF in the continued presence of integrin stretch. The current after DPI was significantly less than the background Cl⁻ current before stretch ($n = 6$, $P < 0.001$). At −100 mV, integrin stretch increased the Cl⁻ current from −0.08 ± 0.02 to −0.29 ± 0.17 pA/pF, and DPI decreased the current to −0.07 ± 0.03 pA/pF. The inward currents were small and were statistically indistinguishable, however. These results suggest that NADPH oxidase is required for both the Cl⁻ SAC and the background Cl⁻ current.

To verify that NADPH oxidase is involved in the regulation of Cl⁻ SAC, the effect of AEBSF, a second NADPH oxidase inhibitor, was examined at two concentrations, 500 μM and 2 mM. AEBSF is structurally distinct from DPI and interferes with the assembly of the active NADPH oxidase complex (Diatchuk et al., 1997).

Experiments with AEBSF are illustrated in Fig. 3. As shown previously, the outwardly rectifying background Cl⁻ current present (Fig. 3, A and D) was increased by 5 min of integrin stretch (Fig. 3, B and D). Treatment with AEBSF (500 μM, 6 min) while maintaining stretch restored the current to its control level (Fig. 3, C and D). At +40 mV, 500 μM AEBSF (5–6 min) blocked 106 ± 7% ($n = 3$, $P = 0.001$) of the Cl⁻ SAC. Stretch significantly increased the outward current from 1.47 ± 0.31 to 2.49 ± 0.52 pA/pF, and 500 μM AEBSF reduced the outward current to 1.43 ± 0.35 pA/pF, a value not different from control. At −100 mV, the effects of integrin stretch and 500 μM AEBSF were small and not statistically significant.

A higher concentration of AEBSF had a more pronounced effect on the Cl⁻ current that was similar to that seen with 60 μM DPI. After the activation of Cl⁻
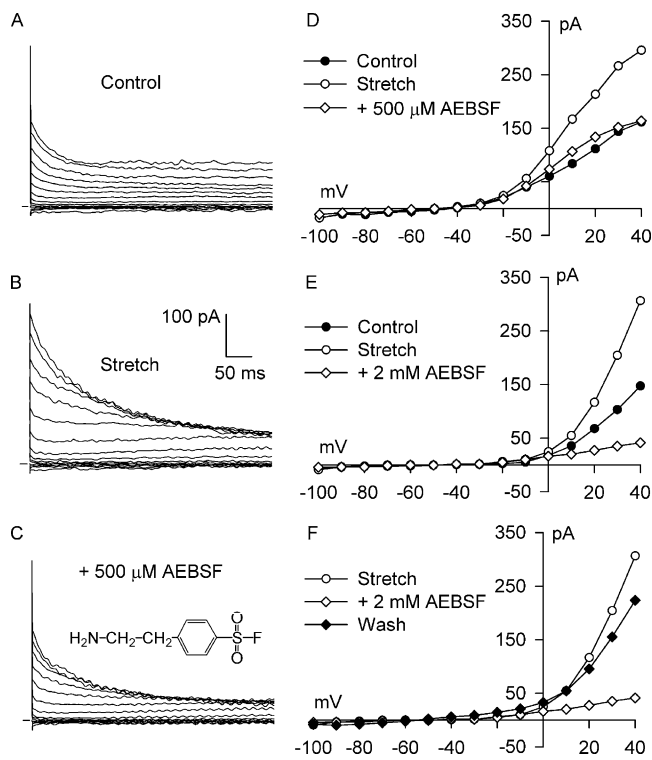
FIGURE 3. AEBSF, an inhibitor of NADPH oxidase assembly and activation, blocks both Cl⁻ SAC and background Cl⁻ current. Currents before (A, Control) and after (B, Stretch) activation of Cl⁻ SAC by 5 min of integrin stretch, and after application of 500 μM AEBSF for 6 min with continued stretch (C, +500 μM AEBSF). Inset, chemical structure of AEBSF. (D) I–V relationships for A–C. Each reversed near E_{Cl}. (E) I–V relationships in a separate experiment during control (●), after Cl⁻ SAC activation by 5 min of integrin stretch (○), and after application of a higher concentration of AEBSF (2 mM) for 6 min with continued stretch (◇). At 2 mM, AEBSF blocked both Cl⁻ SAC and background Cl⁻ current. (F) I–V relationships after integrin stretch and 2 mM AEBSF from E and after a 6-min washout of 2 mM AEBSF with continued stretch. Washout of AEBSF leads to almost complete recovery of Cl⁻ SAC (◆). At +40 mV, AEBSF (500 μM and 2 mM) blocked 106 ± 7% (n = 3) and 139 ± 28% (n = 3) of Cl⁻ SAC, respectively. Block by 2 mM AEBSF was reversed by 91 ± 16% (n = 3) upon washout with continued integrin stretch.

SAC with 5 min of integrin stretch, myocytes were exposed to 2 mM AEBSF for 6 min with continued stretch. This resulted in the complete inhibition of Cl⁻ SAC as well as most of the background Cl⁻ current (Fig. 3 E). At +40 mV, 2 mM AEBSF (5–6 min) reduced the Cl⁻ SAC by 139 ± 28% (n = 3, P = 0.006). In these myocytes, integrin stretch significantly increased the current from 1.22 ± 0.23 to 2.20 ± 0.26 pA/pF, and then 2 mM AEBSF decreased the current to 0.76 ± 0.24 pA/pF.

Block of Cl⁻ current by 2 mM AEBSF was almost completely reversed after 6 min of washout of the drug in the continued presence of integrin stretch (Fig. 3 F). The Cl⁻ current blocked by 2 mM AEBSF at +40 mV recovered by 91 ± 16% (n = 3, P = 0.007), returning
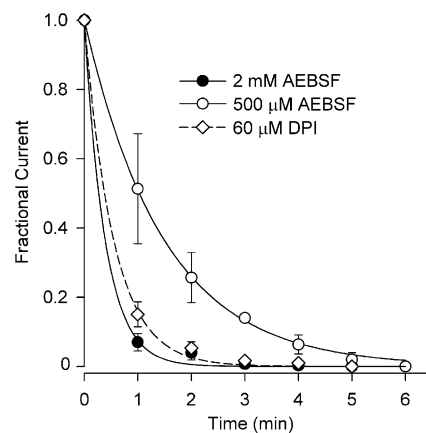

FIGURE 4. Time course of Cl⁻ current block by AEBSF and DPI. Fractional current was determined at 1-min intervals. Block was very rapid and was described by single exponentials with time constants of 1.48 ± 0.17 and 0.39 ± 0.03 for 500 μM and 2 mM AEBSF, respectively, and 0.55 ± 0.03 min, for 60 μM DPI (n = 3).

to 2.01 ± 0.46 pA/pF. There was no significant difference between the stretch-induced current before treatment with AEBSF and after washout (P = 0.496). These results strongly support the idea that NADPH oxidase is required for both the activation of Cl⁻ SAC by integrin stretch and the background Cl⁻ current.

Fig. 4 illustrates the time course of Cl⁻ current block by AEBSF (500 μM and 2 mM) and DPI (60 μM) at +40 mV obtained from I–V curves taken at 1-min intervals. Each is well described by a single exponential. The time constant for Cl⁻ current block by 2 mM AEBSF was 0.39 ± 0.03 min (n = 3), approximately fourfold faster than that for the fourfold lower concentration of AEBSF, 1.48 ± 0.17 min (n = 3). Block of Cl⁻ current by DPI (60 μM) proceeded with a time constant of 0.55 ± 0.03 min (n = 3). The rapid kinetics of block of both the Cl⁻ SAC and the background Cl⁻ current, ∼90% block occurred within 1 min with 2 mM AEBSF and 60 μM DPI, suggests a close coupling between NADPH oxidase activity and gating of the Cl⁻ channels.

Experiments with NADPH oxidase blockers suggest that up-regulation of NADPH oxidase and ultimately the production of O_2^-· and its dismutation to H_2O_2 are critical for the activation of Cl⁻ SAC. If this idea is correct, degradation of the H_2O_2 produced by myocyte stretch should abrogate the response to stretch. Fig. 5 shows the effect of catalase, which rapidly converts H_2O_2 to H_2O, on activation of Cl⁻ SAC by integrin stretch. Following a 15-min exposure of the myocyte to 1,000 U/ml catalase in the bath solution, a control current exhibiting modest outward rectification typical of the background Cl⁻ current was recorded (see Fig. 1 D). Integrin stretch was then applied for 6 min in the continued presence of catalase, a time sufficient to activate significant Cl⁻ SAC, but virtually no change in the
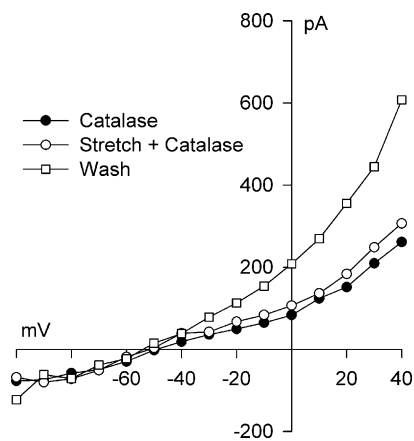
FIGURE 5. Catalase, which rapidly converts H_2O_2 to H_2O, inhibits activation of Cl^- SAC by integrin stretch. I–V relationships before (●) and after (○) 6 min of integrin stretch in the presence of 1,000 U/ml extracellular catalase, and after a 5-min washout of catalase with continued integrin stretch (□). At +40 mV, integrin stretch in the presence of catalase did not significantly activate Cl^- SAC; the Cl^- SAC elicited was 17 ± 7% ($n = 4$; $P = 0.393$) of that in the same cell after washout of catalase.

Cl^- current was observed. Subsequent washout of catalase for 5 min resulted in full activation of Cl^- SAC, documenting the ability of the myocyte to respond to stretch. At +40 mV, in the presence of 1,000 U/ml extracellular catalase, the current after stretch, 1.97 ± 0.42 pA/pF, was not significantly different than that before stretch, 1.77 ± 0.40 pA/pF ($n = 4$, $P = 0.393$). Following washout of catalase, the current markedly increased to 2.86 ± 0.46 pA/pF. The small increment of current activated in the presence of catalase, 0.19 ± 0.08 pA/pF, represented only 17 ± 7% of total Cl^- SAC activated by the end of the catalase washout period.

Angiotensin II Activates a DPI-sensitive, Outwardly Rectifying Cl^- Current

If stretch of β1 integrin releases AngII, which stimulates AT1 receptors in an autocrine–paracrine loop to elicit Cl^- SAC, then exogenous AngII should rapidly elicit a Cl^- current in the absence of stretch. Myocytes were treated with 5 nM AngII for 6 min, a concentration sufficient to activate AT1 (K_d = 420 pM) but not AT2 (K_d = 100 nM) receptors in rabbit ventricle (Wright et al., 1983). As shown in Fig. 6 (A, B, and D), exogenous AngII elicited an outwardly rectifying Cl^- current in the absence of stretch that partially inactivated at positive potentials. Moreover, the AngII-induced current was fully inhibited by the NADPH oxidase blocker DPI (60 μM; Fig. 6, C and D), as previously shown for the stretch-induced Cl^- SAC. At +40 mV, AngII increased the current by 0.85 ± 0.03 pA/pF, from 1.18 ± 0.25 to 2.04 ± 0.27 pA/pF ($n = 4$, $P = 0.01$), and DPI blocked 149 ± 30% of the AngII-induced cur-
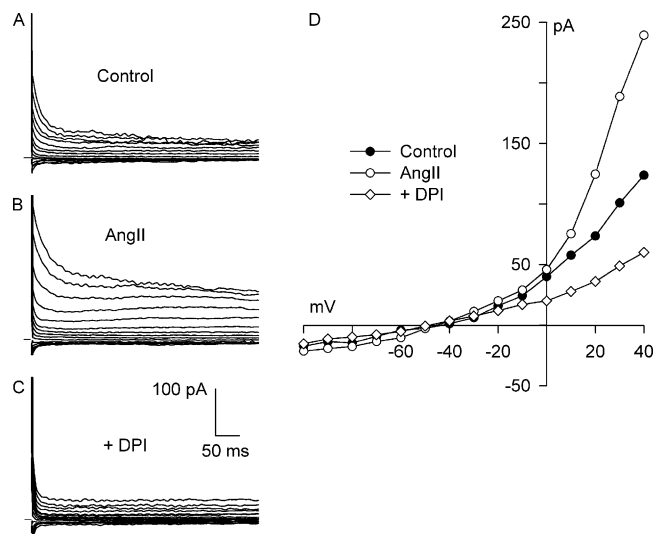

FIGURE 6. Exogenous AngII activates a Cl^- current in the absence of integrin stretch via NADPH oxidase. Currents before (A, Control) and after (B, AngII) a 6-min exposure to 5 nM AngII, and after block of NADPH oxidase by exposure to 60 μM DPI for 5 min in the continued presence of AngII (C, +DPI). (D) I–V relationships for A–C. AngII activated an outwardly rectifying Cl^- current that partially inactivated at positive potentials and reversed at E_{Cl}. DPI rapidly blocked the AngII-induced current and the background Cl^- current. At +40 mV, the AngII-induced Cl^- current was 0.85 ± 0.03 pA/pF ($n = 4$), and DPI blocked this current by 149 ± 30% ($n = 4$).

rent ($n = 4$, $P < 0.005$), reducing the current to 0.75 ± 0.13 pA/pF. There was no significant difference between the background current before AngII and the current after treatment with DPI ($P = 0.11$).

H_2O_2 Activates a Tamoxifen-sensitive, Outwardly Rectifying Cl^- Current

If stretch-induced activation of AT1 receptors and NADPH oxidase stimulates Cl^- current via ROS, exogenous ROS might be expected to mimic the effects of stretch. Fig. 7 illustrates a test of this prediction with H_2O_2 as the ROS. A typical background current was observed under control conditions (Fig. 7, A and E). Addition of 500 μM H_2O_2 to the bath solution leads to the substantial activation of outward Cl^- current in the absence of stretch. The current recorded after a 7-min exposure to H_2O_2 was outwardly rectifying, reversed at −50 mV, and partially inactivated at potentials positive to +10 mV (Fig. 7, B and E), as were shown for the control current. A family of H_2O_2-induced difference currents, calculated by digitally subtracting the control currents from those after application of H_2O_2, and the resulting I–V relationship are shown in Fig. 7 (D and F). H_2O_2 evoked a much greater increase in outward current than inward current, as previously found for integrin stretch, and the difference current reversed at −50 mV, close to the calculated E_{Cl} of −52 mV. Thus,
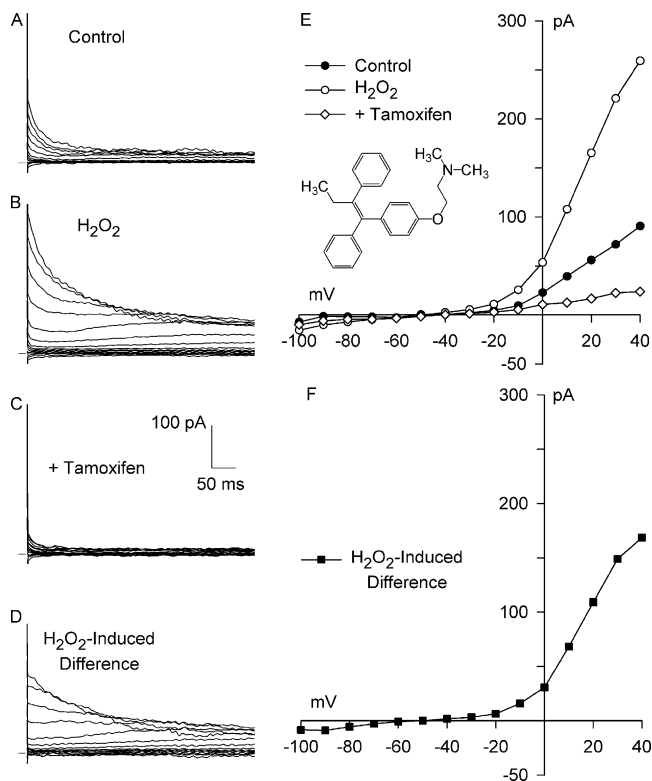
FIGURE 7. Exogenous H_2O_2 activates Cl^- SAC in the absence of integrin stretch. Currents before (A, Control) and after (B, H_2O_2) a 7-min exposure to 500 μM H_2O_2, and after application of 10 μM tamoxifen for 6 min in the continued presence of H_2O_2 (C, +Tamoxifen). The H_2O_2-induced difference current (D, H_2O_2-Induced Difference) was obtained by digital subtraction. (E) I–V relationships for A–C, and for the H_2O_2-induced current (F). Each I–V relationship reversed near E_{Cl}. The H_2O_2-induced current partially inactivated at positive potentials and exhibited strong outward rectification. Tamoxifen, an inhibitor of Cl^- SAC and $I_{Cl,swell}$, blocked all of the H_2O_2-induced Cl^- current, as well as a large fraction of the background Cl^- current. At +40 mV, the H_2O_2-induced Cl^- current was 1.00 ± 0.15 pA/pF ($n = 4$), and tamoxifen blocked this current by 121 ± 15% ($n = 4$). Inset, chemical structure of tamoxifen.

the H_2O_2-induced Cl^- current shares several of the characteristics of both the integrin stretch–induced Cl^- SAC and $I_{Cl,swell}$ (Browe and Baumgarten, 2003b).

Tamoxifen inhibits $I_{Cl,swell}$ but does not affect CFTR or Ca^{2+}-activated Cl^- currents (Hume et al., 2000; Baumgarten and Clemo, 2003). Moreover, tamoxifen inhibits both Cl^- SAC and a large fraction of the background Cl^- current during integrin stretch (Browe and Baumgarten, 2003b). To further identify the H_2O_2-induced current, we tested its sensitivity to tamoxifen. Fig. 7 (C and E) shows that 10 μM tamoxifen, applied for 6 min in the continued presence of 500 μM H_2O_2, completely blocked the Cl^- current elicited by H_2O_2, as well as virtually all of the background Cl^- current.

An H_2O_2-induced, outwardly rectifying Cl^- current that was blocked by 10 μM tamoxifen was observed in

each myocyte tested. H_2O_2 (500 μM), in the absence of integrin stretch, significantly increased outward Cl^- current at +40 mV by 1.00 ± 0.15 pA/pF ($n = 4$, $P < 0.01$), from 1.24 ± 0.21 to 2.27 ± 0.23 pA/pF. Tamoxifen (10 μM, 6–8 min) in the continued presence of H_2O_2 significantly decreased the current at +40 mV to 1.06 ± 0.26 pA/pF, representing a block of 121 ± 15% ($P = 0.002$) of the current evoked by H_2O_2. There was no significant difference between the control current and the current after tamoxifen block ($P = 0.349$). The inward Cl^- current at −100 mV was significantly increased 0.36 ± 0.13 pA/pF ($n = 4$, $P < 0.05$) by H_2O_2, from −0.22 ± 0.08 to −0.59 ± 0.21 pA/pF. Tamoxifen decreased the current at −100 mV to −0.45 ± 0.16 pA/pF in the continued presence of H_2O_2, although block at −100 mV was not statistically significant ($P = 0.2$).

Although 500 μM exogenous H_2O_2 often is used to demonstrate effects of ROS, this concentration may be higher than the local concentration produced by stretch in situ. Fig. 8 compares the activation of outwardly rectifying Cl^- current by different concentrations of exogenous H_2O_2 in the absence of integrin stretch. Exposure to 100 μM H_2O_2 for 7 min increased the outward Cl^- current (Fig. 8 A) to the same degree as seen with 500 μM, whereas exposure to 10 μM H_2O_2 for 7 min elicited a smaller current (Fig. 8 B). At +40 mV, 100 μM H_2O_2 increased Cl^- current by 1.04 ± 0.08 pA/pF, from 1.74 ± 0.15 to 2.78 ± 0.16 pA/pF ($n = 4$; $P < 0.0005$), but 10 μM H_2O_2 stimulated the current by 0.63 ± 0.04 pA/pF ($n = 4$; $P < 0.0005$), from 1.88 ± 0.29 to 2.52 ± 0.33 pA/pF. The current densities at +40 mV for the Cl^- currents activated by 10, 100, and 500 μM H_2O_2 and by integrin stretch are illustrated in Fig. 8 C. The magnitude of the currents evoked by integrin stretch and 100 or 500 μM H_2O_2 were not statistically distinguishable, whereas the Cl^- current elicited by 10 μM H_2O_2 was significantly smaller than the stretch-induced Cl^- SAC ($P = 0.026$).

Fig. 9 compares the kinetics of activation of Cl^- current by 500 μM H_2O_2 and integrin stretch. In both cases, stimulation occurred over several minutes, but differences in the kinetics were notable. The time course for activation of the H_2O_2-induced Cl^- current at +40 mV (Fig. 9 A, filled circles) was well-described by a single exponential with a time constant of 1.79 ± 0.13 min ($n = 4$), equivalent to a $t_{1/2}$ of 1.24 ± 0.09 min. In contrast, the activation of Cl^- SAC at +40 mV (Fig. 9 A, open circles) is sigmoidal with a $t_{1/2}$ of 3.5 ± 0.1 min ($n = 5$) (Browe and Baumgarten, 2003b). The more rapid activation of Cl^- current by H_2O_2 than by stretch is consistent with the idea that H_2O_2 is an intermediate in the process. Moreover, the I–V relationships for the H_2O_2-induced Cl^- current and Cl^- SAC determined after reaching steady-state activation (Fig. 9 B) nearly superimposed.

FIGURE 8. Concentration dependence of H_2O_2-induced current in the absence of integrin stretch. I–V relationships before (●) and after (○) a 7-min exposure to 100 μM (A) or 10 μM (B) exogenous H_2O_2. (C) Comparison of H_2O_2-induced (10, 100, 500 μM) currents at +40 mV (solid bars) with those elicited by integrin stretch (hatched bar). Currents activated by 100 and 500 μM H_2O_2 were not significantly different from each other or from that elicited by integrin stretch, whereas 10 μM H_2O_2 elicited a significantly smaller current than stretch ($P = 0.026$).
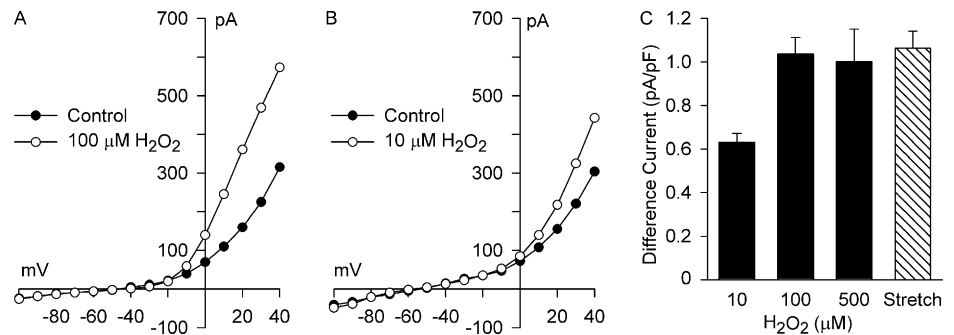
If the action of NADPH oxidase blockers is solely to prevent generation of $O_2^-\cdot$ and ultimately H_2O_2, exogenous H_2O_2 should be sufficient to reactivate the stretch-induced Cl^- current in the presence of NADPH oxidase blockade. Fig. 10 (A and B) illustrates experiments testing this idea. First, myocytes were stretched for 5 min to elicit the Cl^- SAC. Then, either 60 μM DPI (Fig. 10 A) or 500 μM AEBSF (Fig. 10 B) was applied for 5–6 min to block the Cl^- SAC in the continued presence of stretch. Finally, myocytes were exposed to 500 μM H_2O_2 for 10 min in the presence of both the NADPH oxidase blocker and stretch. At +40 mV, H_2O_2 reactivated only $4 \pm 2\%$ ($n = 3$) and $31 \pm 2\%$ ($n = 3$)

of the Cl^- current blocked by DPI and AEBSF, respectively. There was not a significant difference between the current after H_2O_2 addition and the current after either DPI or AEBSF block, however. Thus, block of NADPH oxidase prevented full activation of Cl^- channels by a concentration of exogenous H_2O_2 normally sufficient to fully activate Cl^- SAC.

Tamoxifen blocks both the H_2O_2-induced Cl^- current (Fig. 7) and the stretch-activated Cl^- SAC (Browe and Baumgarten 2003b). Provided that the same channel protein is responsible for both currents, a model assuming block results from binding of tamoxifen to the channel predicts that the kinetics of block of both of these currents will be identical. A test of this prediction
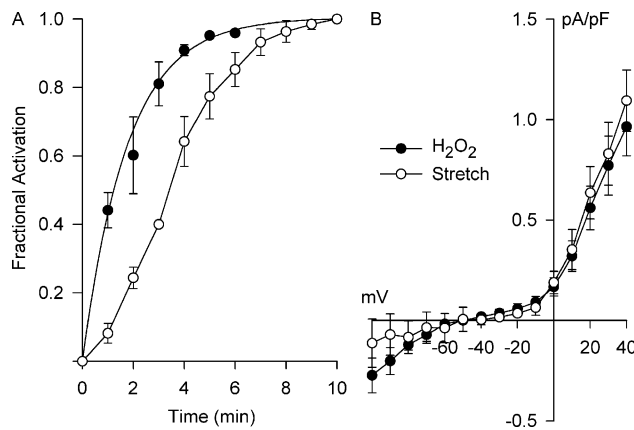

FIGURE 9. Time course for Cl^- SAC activation by H_2O_2 (500 μM) and integrin stretch and their respective steady-state I–V relationships. (A) The H_2O_2- and integrin stretch–induced currents at +40 mV were recorded at 1-min intervals and normalized to the steady-state currents to obtain the fractional activation. The time course for Cl^- SAC activation by H_2O_2 was exponential with a time constant of 1.78 ± 0.13 min ($n = 4$), equivalent to a $t_{1/2}$ of 1.24 ± 0.09 min. Cl^- SAC activation by integrin stretch was slower, following a sigmoidal time course with a $t_{1/2}$ of 3.5 ± 0.1 min ($n = 5$) (Browe and Baumgarten, 2003b). (B) Steady-state I–V relationships for the stretch- and H_2O_2-induced currents could not be distinguished.
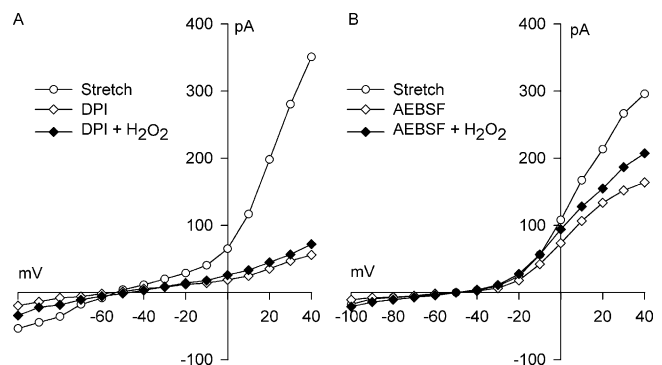

FIGURE 10. Exogenous H_2O_2 does not fully reactivate Cl^- SAC after block of NADPH oxidase by DPI or AEBSF. (A) I–V relationships after Cl^- SAC activation by 5 min of integrin stretch (○), exposure to 60 μM DPI for 5 min with continued stretch (◇), and then application of 500 μM H_2O_2 for 10 min in the continued presence of both integrin stretch and 60 μM DPI (◆). (B) I–V relationships in a similar experiment after Cl^- SAC activation by 5 min of integrin stretch (○), exposure to 500 μM AEBSF for 6 min with continued stretch (◇), and then application of 500 μM H_2O_2 for 10 min in the continued presence of both integrin stretch and 500 μM AEBSF (◆). At +40 mV, H_2O_2 did not reactivate Cl^- SAC after treatment with DPI, $4 \pm 2\%$ ($n = 3$), and only partially reactivated Cl^- SAC, $31 \pm 2\%$ ($n = 3$; $P = 0.104$), after treatment with AEBSF.
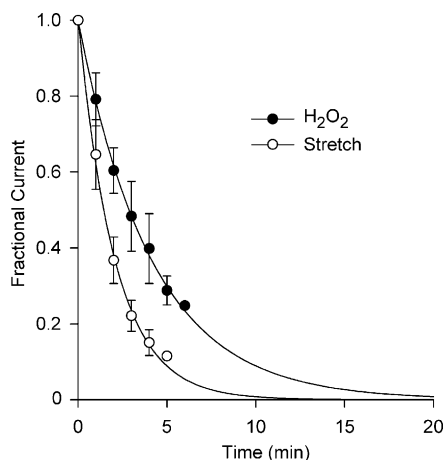
FIGURE 11. Time course of tamoxifen block of H_2O_2- and stretch-induced Cl$^-$ currents. Currents at +40 mV were recorded at 1-min intervals after application of 10 μM tamoxifen and were normalized by the initial current. In both cases, the time course of block was exponential, but the time constant for block of H_2O_2-induced current, 4.15 ± 0.49 min ($n = 4$), was slower than for stretch-induced current, 2.07 ± 0.25 min ($n = 4$, $P < 0.01$). This unexpected discrepancy can be accounted for by an H_2O_2-mediated breakdown of tamoxifen.

is shown in Fig. 11. After 6–8 min of integrin stretch or 7 min of exposure to 500 μM H_2O_2, 10 μM tamoxifen was added in the continued presence of stretch or H_2O_2, respectively, and block at +40 mV was assessed at 1-min intervals. Although block of both the H_2O_2-induced Cl$^-$ current and Cl$^-$ SAC were well described by single exponential functions, the kinetics of block were different. The time constant for tamoxifen block of the H_2O_2-induced Cl$^-$ current, 4.15 ± 0.49 min ($n = 4$), was significantly slower than that of the Cl$^-$ SAC, 2.07 ± 0.25 min ($n = 4$; $P < 0.01$).

DISCUSSION

We previously demonstrated that direct and specific stretch of β1-integrin activates an outwardly rectifying, tamoxifen-sensitive Cl$^-$ SAC in ventricular myocytes via FAK and/or Src and that Cl$^-$ SAC resembles the volume-sensitive Cl$^-$ current, $I_{Cl,swell}$ (Browe and Baumgarten, 2003b). The present results suggest that integrin stretch-induced activation of Cl$^-$ SAC requires release of AngII and subsequent stimulation of both AT1 receptors and sarcolemmal NADPH oxidase. NADPH oxidase directly produces $O_2^-\cdot$, which is rapidly converted to membrane permeant H_2O_2 by dismutation (Brahma-jothi and Campbell, 1999), and H_2O_2 and possibly other ROS participate in the activation of Cl$^-$ SAC. As expected from the proposed mechanism depicted in Fig. 12, inhibition of AT1 receptors by losartan, inhibition of NADPH oxidase by DPI and AEBSF, and scavenging of H_2O_2 by catalase suppressed Cl$^-$ SAC. In addition, exogenous AngII and H_2O_2 each elicited a Cl$^-$ current that resembled Cl$^-$ SAC. The H_2O_2-induced Cl$^-$ current was suppressed by tamoxifen, a blocker of
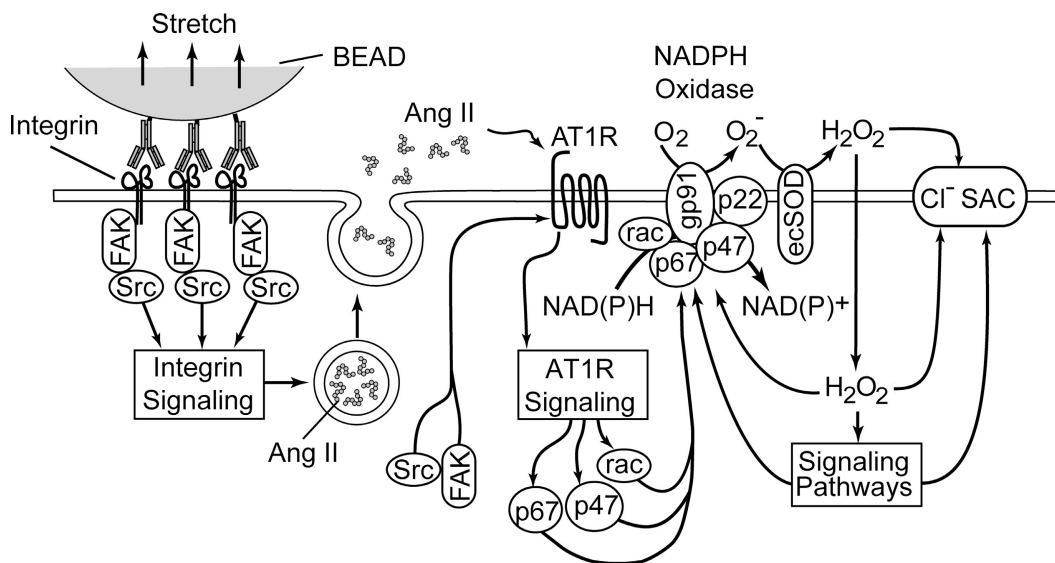

FIGURE 12. Simplified proposed model of the mechanotransduction process coupling β1 integrin stretch to activation of Cl$^-$ SAC in ventricular myocytes. Integrin stretch triggers the phosphorylation and activation of focal adhesion kinase (FAK) and Src, and the release of Ang II from secretory vesicles. Ang II binds to the AT1 receptor (AT1R) and activates the AT1R signaling cascade. Components of the AT1R signaling cascade, possibly in concert with components of integrin signaling, induce the activation of p47^{phox}, p67^{phox}, and rac, which translocate to the membrane and assemble with gp91^{phox} and p22^{phox} to form the active NADPH oxidase complex. NADPH oxidase recruits NAD(P)H as an electron donor and catalyzes the transmembrane transfer of electrons to molecular O_2 to form superoxide (O_2^-). Extracellular $O_2^-\cdot$ is rapidly converted to membrane-permeant H_2O_2 by ecSOD. H_2O_2 may activate Cl$^-$ SAC either directly or via ROS-sensitive signaling pathways. The idea that NADPH oxidase may be a closely coupled regulator of the Cl$^-$ SAC channel is not illustrated.

Cl$^-$ SAC and I$_{Cl,swell}$, and the AngII-induced current was blocked by inhibition of NADPH oxidase. Moreover, the background Cl$^-$ current also was blocked by inhibition of NADPH oxidase but not by an AT1 receptor antagonist. To our knowledge, this is the first report that cardiac Cl$^-$ currents are regulated by H$_2$O$_2$ or other ROS and the first evidence that NADPH oxidase modulates cardiac electrical activity.

Autocrine/Paracrine Regulation of Cl$^-$ SAC by Angiotensin II

AngII is stored in secretory vesicles in myocytes and released within 1 min by mechanical stretch of cultured rat myocytes grown on an elastic substrate (Sadoshima et al., 1993). Stretch-induced AngII release is sufficient to activate AT1 receptors in an autocrine–paracrine loop and induce gene expression and hypertrophy. Block of Cl$^-$ SAC by losartan, a highly selective AT1 antagonist with an IC$_{50}$ of 20 nM (Lambert et al., 1995; Chung and Unger, 1998), activation of Cl$^-$ current by exogenous AngII (5 nM), and the much greater AngII affinity of AT1 than AT2 receptors (Wright et al., 1983) strongly argue for involvement of AngII and AT1 receptors in the transduction of integrin stretch. The amount of AngII released was not determined. It is important to note, however, that a large number of myocytes bound to β1-integrin mAb-coated beads covered the chamber floor. All myocytes were stretched simultaneously, and presumably all released AngII. Therefore the voltage-clamped cell was exposed not only to locally released AngII, but also to AngII delivered by diffusion and solution flow from other cells.

Morita et al. (1995) previously reported that exogenous AngII evokes an outwardly rectifying Cl$^-$ current in rabbit ventricular myocytes. They found the current is blocked by saralasin and eliminated when cytoplasmic free-Ca^{2+} is driven to vanishing levels with Ca^{2+}-free pipette solutions containing 10 mM EGTA. In our study, free-Ca^{2+} was ~35 nM. In rabbit SA node, AngII induces an outwardly rectifying Cl$^-$ current that is PKC dependent and blocked by losartan (Bescond et al., 1994). On the other hand, I$_{CFTR,cardiac}$ is strongly inhibited by AngII via AT1 receptors and inhibition of adenylate cyclase (Obayashi et al., 1997). AngII also activates a Ca^{2+}-dependent Cl$^-$ current in mesangial (Marrero et al., 1996) and adrenal zona fasciculata cells (Chorvatova et al., 1998). In addition to effects on Cl$^-$ currents, AngII modulates a number of cation currents (for review see Chorvatova et al., 1996), and thus, integrin stretch-induced activation of AT1 receptors also may affect cardiac cation currents (Browe and Baumgarten, 2003b).

A coordination of stretch and AngII receptor activation is implicated in a variety of cardiac responses in addition to hypertrophy and gene expression (Sadoshima et al., 1993). Losartan and/or the AngII converting enzyme inhibitor captopril suppress stretch-induced phosphatidylinositol hydrolysis, PKC translocation (Paul et al., 1997), and atrial natriuretic peptide secretion (Ruskoaho et al., 1997). AngII also mediates stretch-induced activation of the Na$^+$/H$^+$ exchanger and changes in contractility in cardiac myocytes (Dostal and Baker, 1998; Cingolani et al., 2001).

Regulation of Cl$^-$ SAC by NADPH Oxidase and ROS

It is proposed that activation of Cl$^-$ SAC by integrin stretch is due to the activation of NADPH oxidase and production of ROS. Involvement of NADPH oxidase and ROS in the stimulation of Cl$^-$ current is supported by three lines of evidence. First, two structurally distinct blockers of NADPH oxidase, DPI and AEBSF, rapidly and completely inhibited Cl$^-$ SAC. DPI acts by displacing FAD from the electron transfer chain (O'Donnell et al., 1993; Doussiere et al., 1999), making it a potent NADPH oxidase inhibitor; its IC$_{50}$ for O$_2^-$· production is 0.9 and 5.6 µM in intact macrophages (Hancock and Jones, 1987) and neutrophils (O'Donnell et al., 1993), respectively. DPI also inhibits other flavoprotein-containing enzymes, however, including nitric oxide synthase (Stuehr et al., 1991). AEBSF prevents assembly of the NADPH oxidase active complex and blocks O$_2^-$· production with an IC$_{50}$ of 1 mM (Diatchuk et al., 1997), but there is no evidence that AEBSF interacts with nitric oxide synthase. Moreover, DPI and AEBSF inhibit ROS-dependent ERK activation in ventricular myocytes (Xiao et al., 2002). Second, activation of Cl$^-$ SAC by integrin stretch was strongly attenuated by extracellular catalase, which rapidly breaks down H$_2$O$_2$. This implies that integrin stretch must lead to H$_2$O$_2$ production and that H$_2$O$_2$ is required for Cl$^-$ SAC activation. The effect of extracellular catalase is consistent with the topology of gp91^{phox} (Nox2), the prototypic phagocyte-type NADPH oxidase found in heart. Nox2 produces O$_2^-$· at the extracellular face of the sarcolemma (Griendling et al., 2000; Vignais, 2002), where ecSOD is positioned to convert O$_2^-$· to H$_2$O$_2$ (Brahmajothi and Campbell, 1999). Third, direct application of exogenous H$_2$O$_2$ in the absence of integrin stretch promptly activated a tamoxifen-sensitive Cl$^-$ current with biophysical characteristics similar to those of Cl$^-$ SAC; the ED$_{50}$ was <10 µM. Although we refer to this as an H$_2$O$_2$-induced Cl$^-$ current, the present data do not exclude the possibility that other reactive species participate in its regulation.

Activation of Cl$^-$ current by H$_2$O$_2$ was more rapid than the activation of Cl$^-$ current by integrin stretch, as expected if H$_2$O$_2$ is an intermediate in stretch-induced signaling. Nevertheless, H$_2$O$_2$ and ROS activate a variety of signaling processes (Allen and Tresini, 2000). We cannot rigorously exclude the possibility that exogenous H$_2$O$_2$ regulates Cl$^-$ current, at least in part, by signaling cascades that are unaffected by integrin stretch.

Both gp91[phox] and Nox4, a homologue of gp91[phox], are found in ventricle (Byrne et al., 2003). Knockout of gp91[phox] abrogates AngII-induced $O_2^-\cdot$ production and ventricular hypertrophy, suggesting gp91[phox] underlies the stretch-induced, NADPH oxidase-dependent responses studied here. It is clear that AngII activates NADPH oxidase in vascular smooth muscle by a process that involves AT1 receptors, FAK and Src, and transactivation of EGF receptors (Seshiah et al., 2002). This may explain why block of FAK and Src inhibits Cl⁻ SAC (Browe and Baumgarten, 2003b). Moreover, in preliminary experiments, we found that Cl⁻ SAC activated by integrin stretch was blocked by the EGF receptor inhibitor AG1478 (unpublished data).

Stretch of cultured rat ventricular myocytes previously was shown to generate $O_2^-\cdot$ by a NADPH-dependent mechanism (Pimentel et al., 2001). Mechanical stimulae activate NADPH oxidase in isolated endothelial cells (Howard et al., 1997; De Keulenaer et al., 1998) and coronary artery denuded of endothelium (Oeckler et al., 2003). NADPH oxidase also is activated by integrin clustering. In eosinophils, CR3 (CD11b/CD18) integrin-mediated adhesion activates NADPH oxidase by a pathway that includes Src, PKC, and PI-3K (Lynch et al., 1999). Application of particles coated with Ab for the α-integrin subunit of LFA-1, CR3, or CR4 (CD11a, CD11b, or CD11c, respectively) or the β2-integrin subunit of CR3 (CD18) stimulates NADPH oxidase in neutrophils by a process that requires cytoskeletal rearrangements but not phagocytosis (Serrander et al., 1999), and activation by anti-β2 integrin Ab depends on PTK (Löfgren et al., 1999).

NADPH oxidase also appeared to be required to support the background Cl⁻ current. The NADPH oxidase inhibitors DPI and AEBSF not only blocked Cl⁻ SAC, but also suppressed the outwardly rectifying component of Cl⁻ current present before integrin stretch. On the other hand, block of the AT1 receptor by losartan did not affect the Cl⁻ current in the absence of stretch. Both gp91[phox] (Nox2) and Nox4 contribute to basal $O_2^-\cdot$ and H_2O_2 production in the unstimulated heart (Bendall et al., 2002; Heymes et al., 2003; Byrne et al., 2003). Therefore, background Cl⁻ current seems to be regulated by NADPH oxidase independent of AT1 receptor activity. Others have attributed the background Cl⁻ current in heart to $I_{Cl,swell}$ (Sorota, 1992; Duan et al., 1995, 1997).

Identity of the H_2O_2-induced Cl⁻ Current

The primary Cl⁻ currents in cardiac myocytes are a PKA-dependent current due to the cardiac isoform of CFTR ($I_{CFTR,cardiac}$), the calcium-dependent transient outward Cl⁻ current ($I_{Cl,Ca}$), and the volume-sensitive Cl⁻ current ($I_{Cl,swell}$) (Hume et al., 2000), and we previously suggested that the Cl⁻ SAC is due to $I_{Cl,swell}$ (Browe and Baumgarten, 2003b). Several of the bio-

physical and pharmacological properties of the H_2O_2-induced current are consistent with Cl⁻ SAC rather than either $I_{CFTR,cardiac}$ or $I_{Cl,Ca}$. Cl⁻ SAC and the H_2O_2-induced current both exhibit strong outward rectification, similar kinetics and voltage-dependence of inactivation, and steady-state I–V curves that are superimposable. $I_{CFTR,cardiac}$ is time independent at all voltages (Shuba et al., 1996; Hume et al., 2000), whereas H_2O_2-induced current partially inactivated at positive potentials. $I_{Cl,Ca}$ is initiated by elevation of cytoplasmic Ca^{2+} and exhibits both inactivation at positive potentials and a bell-shaped I–V relationship if Ca^{2+} handling is uncompromised (Zygmunt and Gibbons, 1991). When cytoplasmic Ca^{2+} is set at an elevated level, however, $I_{Cl,Ca}$ is time independent with a linear I–V relationship (Zygmunt, 1994). In contrast, the H_2O_2-induced current inactivated and displayed outward rectification in Ca^{2+}-free bathing media with strongly buffered pipette Ca^{2+}, conditions that reduced cytoplasmic free-Ca^{2+} to ∼35 nM and minimized Ca^{2+} transients. Moreover, tamoxifen completely blocked the H_2O_2-induced current, but $I_{CFTR,cardiac}$ (Vandenberg et al., 1994) and $I_{Cl,Ca}$ (Valverde et al., 1993) are insensitive to tamoxifen.

One argument against the H_2O_2-induced current being the same as Cl⁻ SAC is the kinetics of block by 10 μM tamoxifen. The time constant was 4.1 min for the H_2O_2-induced current and 2.1 min for the Cl⁻ SAC, whereas identical kinetics were expected if tamoxifen blocked at the same site in both cases. The action of tamoxifen is more complex than classic channel block, however. Tamoxifen can act as an ROS scavenger (Custodio et al., 1994). This suggests that the approximately twofold slowing of block could have arisen because approximately half of the tamoxifen was converted to an inactive form by exposure to 500 μM H_2O_2. In addition, tamoxifen is reported to inhibit NADPH oxidase in uterine smooth muscle (Jain et al., 1999). Because both NADPH oxidase and ROS regulate Cl⁻ SAC/$I_{Cl,swell}$, these actions of tamoxifen are likely to contribute to its block of both Cl⁻ SAC with integrin stretch and $I_{Cl,swell}$ with osmotic swelling.

H_2O_2 modulates multiple Cl⁻ conductances in other systems. It activates native $I_{Cl(Ca)}$ in *Xenopus* oocytes indirectly via Na^+–Ca^{2+} exchange (Schlief and Heinemann, 1995), but suppresses a chlorotoxin-sensitive, time-independent Cl⁻ conductance in retinal pigmented epithelium (Weng et al., 2002), and a sarcoplasmic reticulum Cl⁻ channel (Kourie, 1997). Because the present studies were done under Na^+-free conditions, stimulation of $I_{Cl(Ca)}$ via Na^+–Ca^{2+} exchange can be excluded.

Is NADPH Oxidase Directly Coupled to Cl⁻ Channels?

Inhibition of Cl⁻ SAC and background Cl⁻ current by 60 μM DPI and 2 mM AEBSF was both complete and

rapid. The kinetics of block appears to place a limit on the complexity of the signaling pathway between NADPH oxidase and the Cl^- channel. One possibility is that NADPH oxidase is a closely coupled Cl^- channel regulator. That is to say, it may regulate Cl^- SAC by a direct molecular interaction, as well as by production of ROS. Such a coupling might explain why exogenous H_2O_2 did not fully reactivate Cl^- SAC in the presence of either DPI or AEBSF. Interestingly, recent studies demonstrated that knockout of ClC-3, which has been postulated to underlie cardiac $I_{Cl,swell}$ (Duan et al., 1999), leads to suppression of Nox 2 activity in stimulated leukocytes (Moreland et al., 2004) but up-regulation of Nox1 in vascular smooth muscle (Miller et al., 2004). In addition, β2 integrin cross-linking can trigger a Cl^- efflux that regulates the generation of ROS in neutrophils (Menegazzi et al., 1999).

An alternative possibility is that NADPH oxidase blockers directly inhibit Cl^- channels independent of their action on NADPH oxidase. This possibility seems unlikely because DPI and AEBSF are structurally distinct molecules. Apocynin, a third structurally distinct NADPH oxidase blocker, and DPI also inhibit swelling-induced $I_{Cl,swell}$ in rabbit ventricular myocytes (Ren, Z., personal communication; unpublished data). Moreover, the hypothesis that NADPH oxidase blockers directly inhibit Cl^- channels fails to explain why extracellular catalase abrogated the response to stretch or why exogenous H_2O_2 mimicked stretch by eliciting a Cl^- current. Nevertheless, precise understanding of the relationship between NADPH oxidase and the Cl^- channel and the action of NADPH oxidase blockers awaits further investigation.

NADPH Oxidase, Cl^- Current, and Cardiac Pathophysiology

$I_{Cl,swell}$ blockers reportedly abolish ischemia-, drug-, and hypoosmotic stress–induced preconditioning and exert protective effects in ischemia/reperfusion (for review see Baumgarten and Clemo, 2003). Mohazzab-H et al. (1997) demonstrated that NADPH oxidase is activated during ischemia/reperfusion, and it is well established that H_2O_2 and ROS are critically important in preconditioning (LeBuffe et al., 2003), myocardial injury (Li and Jackson, 2002), and apoptosis (von Harsdorf et al., 1999). As noted above, NADPH oxidase can be blocked and ROS can be scavenged by agents that also block $I_{Cl,swell}$, such as tamoxifen (Jain et al., 1999) and DIDS (Schwingshackl et al., 2000). Indeed, block of NADPH oxidase or scavenging of ROS by such agents, rather than a direct block of Cl^- SAC or $I_{Cl,swell}$, may contribute to their effects on preconditioning, oxidant injury and apoptosis. Alternatively, a functional coupling between NADPH oxidase and Cl^- channels may lead to inhibition of NADPH oxidase when Cl^- channels are blocked.

NADPH oxidase and $I_{Cl,swell}$ are concurrently up-regulated by chronic cardiac disease in animal models and man. Hypertrophy and heart failure trigger increased NADPH-dependent, DPI-inhibitable $O_2^-\cdot$ production due either to increased expression of NADPH oxidase subunits (Li et al., 2002) or increased translocation (Heymes et al., 2003), as well as chronic activation of $I_{Cl,swell}$ (Clemo et al., 1999). Furthermore, increased expression of NADPH oxidase subunits (Fukui et al., 2001; Krijnen et al., 2003) and chronic activation of $I_{Cl,swell}$ (Clemo et al., 2001) are found in the infarct and peri-infarct zones after acute myocardial infarction. The degree to which up-regulation of NADPH oxidase accounts for concurrent up-regulation of $I_{Cl,swell}$ under these conditions is unclear, however.

NADPH Oxidase, ROS, and Cation Channels

The stretch-induced activation of NADPH oxidase and production of ROS also may help explain two other consequences of β1 integrin stretch in rabbit ventricular myocytes: activation of a nonselective cation current and inhibition of the inward rectifier, I_{K1} (Browe and Baumgarten, 2003b). ROS and oxidant stress activate a nonselective cation current (Matsuura and Shattock, 1991; Jabr and Cole, 1995) and inhibit I_{K1} (Matsuura and Shattock, 1991; Jabr and Cole, 1993) in ventricular myocytes. Other cation channels also are modulated by ROS (Kourie, 1998).

In summary, direct and specific stretch of β1 integrin elicits Cl^- SAC in ventricular myocytes by a mechanism that involves release of AngII, engagement of AT1 receptors in an autocrine/paracrine loop, activation of NADPH oxidase, and production of ROS. AngII or H_2O_2 applied exogenously in the absence of stretch also activates Cl^- SAC.

REFERENCES

Allen, R.G., and M. Tresini. 2000. Oxidative stress and gene regulation. *Free Radic. Biol. Med.* 28:463–499.

Baumgarten, C.M., and H.F. Clemo. 2003. Swelling-activated chloride channels in cardiac physiology and pathophysiology. *Prog. Biophys. Mol. Biol.* 82:25–42.

Bendall, J.K., A.C. Cave, C. Heymes, N. Gall, and A.M. Shah. 2002. Pivotal role of a gp91[phox]-containing NADPH oxidase in angiotensin II-induced cardiac hypertrophy in mice. *Circulation.* 105:293–296.

Bescond, J., P. Bois, J. Petit-Jacques, and J. Lenfant. 1994. Characterization of an angiotensin-II-activated chloride current in rabbit sino-atrial cells. *J. Membr. Biol.* 140:153–161.

Bokoch, G.M., and B.A. Diebold. 2002. Current molecular models for NADPH oxidase regulation by Rac GTPase. *Blood*. 100:2692–2696.

Brahmajothi, M.V., and D.L. Campbell. 1999. Heterogeneous basal expression of nitric oxide synthase and superoxide dismutase isoforms in mammalian heart: implications for mechanisms governing indirect and direct nitric oxide-related effects. *Circ. Res.* 85: 575–587.

Browe, D.M., and C.M. Baumgarten. 2003a. Angiotensin (AT1) receptors and sarcolemmal NADPH oxidase regulate a Cl^- current elicited by $\beta 1$ integrin stretch in rabbit ventricular myocytes. *J. Gen. Physiol.* 122:31a (Abstract).

Browe, D.M., and C.M. Baumgarten. 2003b. Stretch of $\beta 1$ integrin activates an outwardly-rectifying chloride current via FAK and Src in rabbit ventricular myocytes. *J. Gen. Physiol.* 122:689–702.

Browe, D.M., and C.M. Baumgarten. 2004. Angiotensin II (AT1) receptors and NADPH oxidase regulate a Cl^- current elicited by $\beta 1$ integrin stretch in ventricular myocytes. *Biophys. J.* 86:545a (Abstract).

Byrne, J.A., D.J. Grieve, J.K. Bendall, J.M. Li, C. Grove, J.D. Lambeth, A.C. Cave, and A.M. Shah. 2003. Contrasting roles of NADPH oxidase isoforms in pressure-overload versus angiotensin II-induced cardiac hypertrophy. *Circ. Res.* 93:802–805.

Chorvatova, A., N. Gallo-Payet, C. Casanova, and M.D. Payet. 1996. Modulation of membrane potential and ionic currents by the AT1 and AT2 receptors of angiotensin II. *Cell. Signal.* 8:525–532.

Chorvatova, A., A. Guyot, C. Ojeda, O. Rougier, and A. Bilbaut. 1998. Activation by angiotensin II of Ca^{2+}-dependent K^+ and Cl^- currents in zona fasciculata cells of bovine adrenal gland. *J. Membr. Biol.* 162:39–50.

Chung, O., and T. Unger. 1998. Pharmacology of angiotension receptors and AT_1 receptor blockers. *Basic Res. Cardiol.* 93:15–23.

Cingolani, H.E., N.G. Perez, and M.C. Camilion de Hurtado. 2001. An autocrine/paracrine mechanism triggered by myocardial stretch induces changes in contractility. *News Physiol. Sci.* 16:88–91.

Clemo, H.F., B.S. Stambler, and C.M. Baumgarten. 1999. Swelling-activated chloride current is persistently activated in ventricular myocytes from dogs with tachycardia-induced congestive heart failure. *Circ. Res.* 84:157–165.

Clemo, H.F., J. Rana, A.M. Vaida, G.N. Tseng, R.S. Higgins, and C.M. Baumgarten. 2001. Chronic activation of $I_{Cl,swell}$ in canine infarction model suppresses inducibility of early afterdepolarizations. *Circulation*. 104:II-624 (Abstract).

Custodio, J.B., T.C. Dinis, L.M. Almeida, and V.M. Madeira. 1994. Tamoxifen and hydroxytamoxifen as intramembraneous inhibitors of lipid peroxidation. Evidence for peroxyl radical scavenging activity. *Biochem. Pharmacol.* 47:1989–1998.

De Keulenaer, G.W., D.C. Chappell, N. Ishizaka, R.M. Nerem, R.W. Alexander, and K.K. Griendling. 1998. Oscillatory and steady laminar shear stress differentially affect human endothelial redox state. *Circ. Res.* 82:1094–1101.

Diatchuk, V., O. Lotan, V. Koshkin, P. Wikstroem, and E. Pick. 1997. Inhibition of NADPH oxidase activation by 4-(2-aminoethyl)-benzenesulfonyl fluoride and related compounds. *J. Biol. Chem.* 272:13292–13301.

Dostal, D.E., and K.M. Baker. 1998. Angiotensin and endothelin: messengers that couple ventricular stretch to the Na^+/H^+ exchanger and cardiac hypertrophy. *Circ. Res.* 83:870–873.

Doussiere, J., J. Gaillard, and P.V. Vignais. 1999. The heme component of the neutrophil NADPH oxidase complex is a target for aryliodonium compounds. *Biochemistry*. 38:3694–3703.

Duan, D., B. Fermini, and S. Nattel. 1995. Alpha-adrenergic control of volume-regulated Cl^- currents in rabbit atrial myocytes. Characterization of a novel ionic regulatory mechanism. *Circ. Res.* 77:

379–393.

Duan, D., J.R. Hume, and S. Nattel. 1997. Evidence that outwardly rectifying Cl^- channels underlie volume-regulated Cl currents in heart. *Circ. Res.* 80:103–113.

Duan, D., S. Cowley, B. Horowitz, and J.R. Hume. 1999. A serine residue in ClC-3 links phosphorylation- dephosphorylation to chloride channel regulation by cell volume. *J. Gen. Physiol.* 113: 57–70.

Fukui, T., M. Yoshiyama, A. Hanatani, T. Omura, J. Yoshikawa, and Y. Abe. 2001. Expression of p22-phox and gp91-phox, essential components of NADPH oxidase, increases after myocardial infarction. *Biochem. Biophys. Res. Commun.* 281:1200–1206.

Grandvaux, N., S. Elsen, and P.V. Vignais. 2001. Oxidant-dependent phosphorylation of p40phox in B lymphocytes. *Biochem. Biophys. Res. Commun.* 287:1009–1016.

Griendling, K.K., and M. Ushio-Fukai. 2000. Reactive oxygen species as mediators of angiotensin II signaling. *Regul. Pept.* 91:21–27.

Griendling, K.K., D. Sorescu, and M. Ushio-Fukai. 2000. NAD(P)H oxidase role in cardiovascular biology and disease. *Circ. Res.* 86: 494–501.

Hagiwara, N., H. Masuda, M. Shoda, and H. Irisawa. 1992. Stretch-activated anion currents of rabbit cardiac myocytes. *J. Physiol.* 456:285–302.

Hancock, J.T., and O.T. Jones. 1987. The inhibition by diphenyl-eneiodonium and its analogues of superoxide generation by macrophages. *Biochem. J.* 242:103–107.

Heymes, C., J.K. Bendall, P. Ratajczak, A.C. Cave, J.L. Samuel, G. Hasenfuss, and A.J. Shah. 2003. Increased myocardial NADPH oxidase activity in human heart failure. *J. Am. Coll. Cardiol.* 41: 2164–2171.

Howard, A.B., R.W. Alexander, R.M. Nerem, K.K. Griendling, and W.R. Taylor. 1997. Cyclic strain induces an oxidative stress in endothelial cells. *Am. J. Physiol. Cell Physiol.* 272:C421–C427.

Hume, J.R., D. Duan, M.L. Collier, J. Yamazaki, and B. Horowitz. 2000. Anion transport in heart. *Physiol. Rev.* 80:31–81.

Jabr, R.I., and W.C. Cole. 1993. Alterations in electrical activity and membrane currents induced by intracellular oxygen-derived free radical stress in guinea pig ventricular myocytes. *Circ. Res.* 72: 1229–1244.

Jabr, R.I., and W.C. Cole. 1995. Oxygen-derived free radical stress activates nonselective cation current in guinea pig ventricular myocytes. Role of sulfhydryl groups. *Circ. Res.* 76:812–824.

Jain, S., D. Saxena, P.G. Kumar, S.S. Koide, and M. Laloraya. 1999. Effect of estradiol and selected antiestrogens on pro- and antioxidant pathways in mammalian uterus. *Contraception*. 60:111–118.

Kourie, J.I. 1997. A redox O_2 sensor modulates the SR Ca^{2+} countercurrent through voltage- and Ca^{2+}-dependent Cl^- channels. *Am. J. Physiol. Cell Physiol.* 272:C324–C332.

Kourie, J.I. 1998. Interaction of reactive oxygen species with ion transport mechanisms. *Am. J. Physiol.* 275:C1–C24.

Krijnen, P.A.J., C. Meischl, C.E. Hack, C.J.L.M. Meijer, C.A. Visser, D. Roos, and H.W.M. Niessen. 2003. Increased Nox2 expression in human cardiomyocytes after acute myocardial infarction. *J. Clin. Pathol.* 56:194–199.

Lambert, C., Y. Massillon, and S. Meloche. 1995. Upregulation of cardiac angiotensin II AT1 receptors in congenital cardiomyopathic hamsters. *Circ. Res.* 77:1001–1007.

LeBuffe, G., P.T. Schumacker, Z.H. Shao, T. Anderson, H. Iwase, and T.L. Vanden Hoek. 2003. ROS and NO trigger early preconditioning: relationship to mitochondrial K_{ATP} channel. *Am. J. Physiol. Heart Circ. Physiol.* 284:H299–H308.

Lepple-Wienhues, A., I. Szabo, U. Wieland, L. Heil, E. Gulbins, and F. Lang. 2000. Tyrosine kinases open lymphocyte chloride channels. *Cell. Physiol. Biochem.* 10:307–312.

Li, C., and R.M. Jackson. 2002. Reactive species mechanisms of cellular hypoxia-reoxygenation injury. *Am. J. Physiol. Cell Physiol.* 282: C227–C241.

Li, J.M., N.P. Gall, D.J. Grieve, M. Chen, and A.M. Shah. 2002. Activation of NADPH oxidase during progression of cardiac hypertrophy to failure. *Hypertension.* 40:477–484.

Li, W.G., F.J. Miller Jr., H.J. Zhang, D.R. Spitz, L.W. Oberley, and N.L. Weintraub. 2001. H_2O_2-induced O_2^- production by a non-phagocytic NAD(P)H oxidase causes oxidant injury. *J. Biol. Chem.* 276:29251–29256.

Löfgren, R., L. Serrander, M. Forsberg, Å. Wilsson, Å. Wasteson, and O. Stendahl. 1999. CR3, FcγRIIA, and FcγRIIIA induce activation of the respiratory burst in human neutrophils: the role of intracellular Ca^{2+}, phospholipase D and tyrosine phosphorylation. *Biochim. Biophys. Acta.* 1452:46–59.

Lynch, O.T., M.A. Giembycz, P.J. Barnes, P.G. Hellewell, and M.A. Lindsay. 1999. 'Outside-in' signaling mechanisms underlying CD11b/CD18-mediated NADPH oxidase activation in human adherent blood eosinophils. *Br. J. Pharmacol.* 128:1149–1158.

Marrero, M.B., B. Schieffer, H. Ma, K.E. Bernstein, and B.N. Ling. 1996. ANG II-induced tyrosine phosphorylation stimulates phospholipase C-γ1 and Cl-channels in mesangial cells. *Am. J. Physiol. Cell Physiol.* 270:C1834–C1842.

Matsuura, H., and M.J. Shattock. 1991. Effects of oxidant stress on steady-state background currents in isolated ventricular myocytes. *Am. J. Physiol. Heart Circ. Physiol.* 261:H1358–H1365.

Menegazzi, R., S. Busetto, E. Decleva, R. Cramer, P. Dri, and P. Patriarca. 1999. Triggering of chloride ion efflux from human neutrophils as a novel function of leukocyte β2 integrins: relationship with spreading and activation of the respiratory burst. *J. Immunol.* 162:423–434.

Miller, F.J., Jr., A.H. Chamseddine, T.J. Barna, and F.S. Lamb. 2004. Role of ClC3 chloride channels in intracellular superoxide levels and cell growth. *FASEB J.* 18:A311–A312 (Abstract).

Mohazzab-H, K.M., P.M. Kaminski, and W.S. Wolin. 1997. Lactate and PO2 modulate superoxide anion production in bovine cardiac myocytes: potential role of NADH oxidase. *Circulation.* 96: 614–620.

Morita, H., J. Kimura, and M. Endoh. 1995. Angiotensin II activation of a chloride current in rabbit cardiac myocytes. *J. Physiol.* 483:119–130.

Moreland, J.G., W.M. Nauseef, A.P. Davis, G. Bailey, and F.S. Lamb. 2004. ClC-3 chloride channel is involved in generation of the respiratory burst by stimulated leukocytes. *FASEB J.* 18:A1158 (Abstract).

Nilius, B., T. Voets, J. Prenen, H. Barth, K. Aktories, K. Kaibuchi, G. Droogmans, and J. Eggermont. 1999. Role of rho and rho kinase in the activation of volume-regulated anion channels in bovine endothelial cells. *J. Physiol.* 516:67–74.

Obayashi, K., M. Horie, L.H. Xie, K. Tsuchiya, A. Kubota, H. Ishida, and S. Sasayama. 1997. Angiotensin II inhibits protein kinase A-dependent chloride conductance in heart via pertussis toxin-sensitive G proteins. *Circulation.* 95:197–204.

O'Donnell, V.B., D.G. Tew, O.T.G. Jones, and P.J. England. 1993. Studies on the inhibitory mechanism of iodonium compounds with special reference to neutrophil NADPH oxidase. *Biochem. J.* 290:41–49.

Oeckler, R.A., P.M. Kaminski, and M.S. Wolin. 2003. Stretch enhances contraction of bovine coronary arteries via an NAD(P)H oxidase -mediated activation of the extracellular signal-regulated kinase mitogen-activated protein kinase cascade. *Circ. Res.* 92:23–31.

Parsons, J.T. 2003. Focal adhesion kinase: the first ten years. *J. Cell Sci.* 116:1409–1416.

Paul, K., N.A. Ball, G.W. Dorn II, and R.A. Walsh. 1997. Left ventric-

ular stretch stimulates angiotensin II-mediated phosphatidylinositol hydrolysis and protein kinase C epsilon isoform translocation in adult guinea pig hearts. *Circ. Res.* 81:643–650.

Pimentel, D.R., J.K. Amin, L. Xiao, T. Miller, J. Viereck, J. Oliver-Krasinski, R. Baliga, J. Wang, D.A. Siwik, K. Singh, et al. 2001. Reactive oxygen species mediate amplitude-dependent hypertrophic and apoptotic responses to mechanical stretch in cardiac myocytes. *Circ. Res.* 89:453–460.

Ross, R.S., and T.K. Borg. 2001. Integrins and the myocardium. *Circ. Res.* 88:1112–1119.

Ruskoaho, H., H. Leskinen, J. Magga, P. Taskinen, P. Mantymaa, O. Vuolteenaho, and J. Leppaluoto. 1997. Mechanisms of mechanical load-induced atrial natriuretic peptide secretion: role of endothelin, nitric oxide, and angiotensin II. *J. Mol. Med.* 75:876–885.

Sadoshima, J., and S. Izumo. 1997. The cellular and molecular response of cardiac myocytes to mechanical stress. *Annu. Rev. Physiol.* 59:551–571.

Sadoshima, J., Y. Xu, H.S. Slayter, and S. Izumo. 1993. Autocrine release of angiotensin II mediates stretch-induced hypertrophy of cardiac myocytes in vitro. *Cell.* 75:977–984.

Schlief, T., and S.H. Heinemann. 1995. H_2O_2-induced chloride currents are indicative of an endogenous Na^+-Ca^{2+} exchange mechanism in *Xenopus* oocytes. *J. Physiol.* 486:123–130.

Schwingshackl, A., R. Moqbel, and M. Duszyk. 2000. Involvement of ion channels in human eosinophil respiratory burst. *J. Allergy Clin. Immunol.* 106:272–279.

Serrander, L., J. Larsson, H. Lundqvist, M. Lindmark, M. Fällman, C. Dahlgren, and O. Stendahl. 1999. Particles binding β2-integrins mediate intracellular production of oxidative metabolites in human neutrophils independently of phagocytosis. *Biochim. Biophys. Acta.* 1452:133–144.

Seshiah, P.N., D.S. Weber, P. Rocic, L. Valppu, Y. Taniyama, and K.K. Griendling. 2002. Angiotensin II stimulation of NAD(P)H oxidase activity: upstream mediators. *Circ. Res.* 91:406–413.

Shi, C., S. Barnes, M. Coca-Prados, and M.E.M. Kelly. 2002. Protein tyrosine kinase and protein phosphatase signaling pathways regulate volume-sensitive chloride currents in a nonpigmented ciliary epithelial cell line. *Invest. Ophthalmol. Vis. Sci.* 43:1525–1532.

Shuba, L.M., T. Ogura, and T.F. McDonald. 1996. Kinetic evidence distinguishing volume-sensitive chloride current from other types in guinea pig ventricular myocytes. *J. Physiol.* 491:69–80.

Sorota, S. 1992. Swelling-induced chloride-sensitive current in canine atrial cells revealed by whole-cell patch-clamp method. *Circ. Res.* 70:679–687.

Sorota, S. 1995. Tyrosine protein kinase inhibitors prevent activation of cardiac swelling-induced chloride current. *Pflugers Arch.* 431:178–185.

Stuehr, C., O.A. Fasehun, N.S. Kwon, S.S. Gross, J.A. Gonzalez, R. Levi, and C.F. Nathan. 1991. Inhibition of macrophage and endothelial cell nitric oxide synthase by diphenyleneiodonium and its analogues. *FASEB J.* 5:98–103.

Tilly, B.C., M.J. Edixhoven, L.G. Tertoolen, N. Morii, Y. Saitoh, S. Narumiya, and H.R. de Jonge. 1996. Activation of the osmo-sensitive chloride conductance involves p21rho and is accompanied by a transient reorganization of the F-actin cytoskeleton. *Mol. Biol. Cell.* 7:1419–1427.

Touyz, R.M. 2002. Recent advances in angiotensin II signaling. *Braz. J. Med. Biol. Res.* 35:1001–1015.

Tseng, G.N. 1992. Cell swelling increases membrane conductance of canine cardiac cells: evidence for a volume-sensitive Cl channel. *Am. J. Physiol.* 262:C1056–C1068.

Valverde, M.A., G.M. Mintenig, and F.V. Sepulveda. 1993. Differential effects of tamoxifen and I^- on three distinguishable chloride currents activated in T84 intestinal cells. *Pflugers Arch.* 425:552–

554.

Vandenberg, J.I., A. Yoshida, K. Kirk, and T. Powell. 1994. Swelling-activated and isoprenaline-activated chloride currents in guinea pig cardiac myocytes have distinct electrophysiology and pharmacology. *J. Gen. Physiol.* 104:997–1017.

Vignais, P.V. 2002. The superoxide-generating NADPH oxidase: structural aspects and activation mechanism. *Cell. Mol. Life Sci.* 59:1428–1459.

von Harsdorf, R., P.F. Li, and R. Dietz. 1999. Signaling pathways in reactive oxygen species-induced cardiomyocyte apoptosis. *Circulation.* 99:2934–2941.

Wang, N., J.P. Butler, and D.E. Ingber. 1993. Mechanotransduction across the cell surface and through the cytoskeleton. *Science.* 260:1124–1127.

Weng, T.X., B.F. Godley, G.F. Jin, N.J. Mangini, B.G. Kennedy, A.S.L. Yu, and N.K. Wills. 2002. Oxidant and antioxidant modulation of chloride channels expressed in human retinal pigment epithelium. *Am. J. Physiol. Cell Physiol.* 283:C839–C849.

Wright, G.B., R.W. Alexander, L.S. Ekstein, M.A. Gimbrone, and M.A. Jr. 1983. Characterization of the rabbit ventricular myocardial receptor for angiotensin II. Evidence for two sites of different affinities and specificities. *Mol. Pharmacol.* 24:213–221.

Xiao, L., D.R. Pimentel, J. Wang, K. Singh, W.S. Colucci, and D.B. Sawyer. 2002. Role of reactive oxygen species and NAD(P)H oxidase in α_1-adrenoceptor signaling in adult rat cardiac myocytes. *Am. J. Physiol. Cell Physiol.* 282:C926–C934.

Yamaguchi, M., S. Saeki, H. Yamane, N. Okamura, and S. Ishibashi. 1996. Involvement of several protein kinases in the phosphorylation of p47-phox. *Biochem. Biophys. Res. Commun.* 220:891–895.

Zygmunt, A.C. 1994. Intracellular calcium activates a chloride current in canine ventricular myocytes. *Am. J. Physiol. Heart Circ. Physiol.* 267:H1984–H1995.

Zygmunt, A.C., and W.R. Gibbons. 1991. Calcium-activated chloride current in rabbit ventricular myocytes. *Circ. Res.* 68:424–437.